INTERNATIONAL JOURNAL FOR NUMERICAL METHODS IN FLUIDS, VOL. 19, 181–206 (1994)

AN INTEGRATED MODELLING SYSTEM FOR COASTAL AREA DYNAMICS

K. A. KLEVANNY

Gydroproject Institute, 22 Pr. Ispitatelei, 197227 St. Petersburg, Russia

G. V. MATVEYEV

Nevski Courier Ltd., 7 Nevski Pr., 191065 St. Petersburg, Russia

AND

N. E. VOLTZINGER

Institute of Oceanology, Russian Academy of Sciences, 30 Pervaya Liniya, 199053 St. Petersburg, Russia

SUMMARY

Two-dimensional initial–boundary value problems are considered for the shallow water equations and the equation of advection and dispersion of pollutants. The problems are solved in curvilinear boundary fitted co-ordinates. The transformed equations are integrated on a regular grid by the semi-implicit and implicit finite difference methods. Based on the numerical method, the integrated modelling system *Cardinal* for coastal area dynamics and pollution processes is developed for application on personal computers. Examples of computations are given.

KEY WORDS Boundary-fitted co-ordinates Semi-implicit and implicit finite difference methods Coastal area water dynamics software

1. INTRODUCTION

To describe storm surges, tsunamis, typhoons, tides, seiches, bores, wind-driven circulations, river flows and other natural phenomena, the shallow water equations are used. The classical theory of the shallow water equations is an approximate theory which follows from the assumption that the horizontal scale of the motion, e.g. the wavelength, is much larger than the vertical scale, e.g. the depth of fluid.[1] The shallow water equations are often used with lateral turbulent eddy diffusion terms. The equations thus obtained are of the incompletely parabolic type.[2] The formulation of boundary value problems for these equations differs from that for the shallow water equations of the quasi-hyperbolic type.

One of the major difficulties in solving all the above-mentioned problems is the complex configuration of the integration domain, which corresponds to the real shoreline contour. The widely used approach to numerical modelling of fluid motions is to approximate the boundary of the domain by a series of line segments parallel to the Cartesian co-ordinate axes. A drawback of this approach is that the solution is distorted in the boundary zone, i.e. where, as implied, the most stringent requirements are imposed on the accuracy of the resolution.[3,4] Using a piecewise linear approximation of the boundary in the case where it alternates at each grid step, the boundary condition of zero velocity normal to the boundary is interpreted as a condition

0271–2091/94/150181–26

Received 8 February 1993
Revised 3 August 1993

of zero velocity vector. This leads to an essential error at the points nearest the boundary. Another defect of such an approximation is that it cannot be improved: the perimeter of the computational domain is not varied as the grid is refined, while the relative defect of the metrics can be considerable depending on the coast geometry.

One of the widely used methods for solving boundary value problems in complicated domains is the finite element method.[5] Another approach, the one used here, consists of mapping a given domain on to a canonical one and integrating the modified equations in it by a finite difference method. The accuracy of solutions obtained with these methods is improved. A good illustration of this is given in Reference 6, where a comparison of lines of equal water elevation at the boundary shows that a transition to curvilinear co-ordinates is useful: the errors arising from the stepwise approximation are not removed with the refinement of a rectangular grid. Mapping of a curvilinear grid on to a rectangular one can be implemented in many ways, e.g. by solving the boundary value problem for a set of elliptical equations,[7] as is done in this paper. The given equations transformed to curvilinear co-ordinates are then integratred in a canonical domain with simple boundary conditions.

The curvilinear grid approach developed in computational aerodynamics is now used for solving oceanological and hydrological boundary value problems in multiply connected domains of complex shape. In References 8-13 the shallow water equations are modified to curvilinear co-ordinates, but as unknowns the Cartesian components of velocity remain unchanged.

The present model represents modificiations of the shallow water equations in terms of the contravariant components of flux.[14] It makes the equations simpler and especially simplifies the boundary conditions. Such equations were also used by Sheng,[15] but his form of the advection terms differs from that derived in Reference 14. In his paper the form of the lateral turbulent diffusion terms and the method of solution are not shown.

The modified criterion of stability for explicit shemes in curvilinear co-ordinates depends not only on the fluid depth but also on the metric of transformation. In zones of small-scale geometry and fast flows, defined by the presence of hydrotechnical structures and the morphometry, the time step of numerical integration for explicit schemes can be rather small, of the order of a few seconds. This makes it more reasonable to prefer implicit or semi-implicit methods of integration of the equations in curvilinear co-ordinates. The equations in terms of the contravariant flow components are easy to implement by the semi-implicit method discussed for Cartesian co-ordinates in References 16–18. In the semi-implicit method the level gradients are approximated implicitly and the advection is approximated explicitly. The method does not require matrix inversion for each time step. It is realized by a direct tridiagonal solver for one of the dependent variables on each time half-step and by determination of the other two variables from explicit formulae. With advection neglected, this method is unconditionally stable. In the general case it often allows computation with a Courant–Friedrich–Lewy (CFL) stability criterion large enough such that limitations on the value of the time step are determined only by the requirements of accuracy. To improve the stability of the semi-implicit method, the Euler–Lagrange representation of advection[18] or iterations[19] may be used.

The study of contaminant propagation in the coastal zone is an important problem associated primarily with environmental problems. It is needed to develop pollution transport computational methods, which make it possible to analyse the field of evolution with waste parameter variation under varied hydrometeorological conditions, in order to evaluate different courses of action. For modelling the transport of pollutants with curvilinear co-ordinates it is also reasonable to use implicit finite differences. Of primary importance here is the appropriate approximation of the advection terms for which schemes of high resolution are very useful.[20] For explicit schemes this was shown by Munz.[21]

Considerable experience is being obtained at present in numerical computations of the dynamics and transport of pollutants with curvilinear co-ordinates. At the same time we consider that a discussion centred on the features of computer modelling systems is an important theme.

In the next section we present the derivation of the shallow water equations with viscosity for the contravariant components of flux. The main difficulty here, as well as with Cartesian co-ordinates, lies in the formulation of the open boundary problem. It should be noted that usually it is impossible to impose correct boundary conditions. However, we include a formulation of correct boundary conditions for the hyperbolic and viscous shallow water equations in contravariant co-ordinates. The semi-implicit method for these equations is presented in Section 3. The derivation of the advection–diffusion equation for contravariant flux components is given in Section 4. Section 5 deals with the implicit scheme for the advection–diffusion equation. In the last section examples applications of the model are given. In the Appendix we give a functional description and the basic characteristics of the interactive modelling system *Cardinal* for solving problems of the dynamics and contamination of an arbitrary water area under a wide range of conditions.

2. VERTICALLY AVERAGED EQUATIONS IN CURVILINEAR CO-ORDINATES

Equations for the contravariant components of flux.

In the domain $Q_2 = \{x, y \in \Omega, t \geqslant 0\}$ let us consider the following form of the viscous shallow water equations:

$$U_t + \left(\frac{U^2}{H}\right)_x + \left(\frac{UV}{H}\right)_y + gH\zeta_x = fV + k_w w_{(x)}|\mathbf{w}| - \mu \frac{U|\mathbf{V}|}{H^2} + \mu_l \nabla^2 U - \frac{H}{\rho_0}\frac{\partial p_a}{\partial x}, \tag{1}$$

$$V_t + \left(\frac{UV}{H}\right)_x + \left(\frac{V^2}{H}\right)_y + gH\zeta_y = -fU + k_w w_{(y)}|\mathbf{w}| - \mu \frac{V|\mathbf{V}|}{H^2} + \mu_l \nabla^2 V - \frac{H}{\rho_0}\frac{\partial p_a}{\partial y}, \tag{2}$$

$$\zeta_t + U_x + V_y = \omega_s, \tag{3}$$

where $U = \int_{-h}^{\zeta} u\,dz$, $V = \int_{-h}^{\zeta} v\,dz$, u and v are the Cartesian components of the velocity vector, ζ is the surface elevation, $H = h + \zeta$, $h = h(x, y)$ is the undisturbed depth, f is the Coriolis parameter, k_w is the wind friction coefficient, $w_{(x)}$ and $w_{(y)}$ are the Cartesian components of the wind velocity vector $\mathbf{w}$, μ is the bottom friction coefficient, $\mathbf{V}$ is the flux vector, p_a is the atmospheric pressure, g is the gravitational acceleration, μ_l is the lateral turbulent eddy coefficient and ω_s is the internal water source discharge per unit area.

As shown by Gustafsson and Sundström,[2] correct boundary conditions for equations (1)–(3) may have the form (e.g. for x = const. boundary)

$$U = 0 \quad \text{and} \quad \theta V + (1-\theta)\mu_l V_x/\sqrt{(gh)} = \gamma_1, \quad 0 \leq \theta \leq 1, \quad \text{on the solid boundary,} \tag{4}$$

$$U + \sqrt{(gh)}\zeta = \gamma_2, \quad V = \gamma_3 \quad \text{and} \quad \mu_l U_x = \gamma_4 \quad \text{on the inflow boundary,} \tag{5}$$

$$U - \sqrt{(gh)}\zeta + \mu_l U_x/\sqrt{(gh)} = \gamma_5 \quad \text{and} \quad \mu_l V_x = \gamma_6 \quad \text{on the outflow boundary,} \tag{6}$$

where $\gamma_i(t)$ are arbitrary functions. These conditions remain valid for the hyperbolic shallow water equations, i.e. for the case $\mu_l \to 0$.[22]

Let us introduce curvilinear co-ordinates $\xi(x, y)$ and $\eta(x, y)$ concordant with the configuration of the given domain $\Omega(x, y)$: on a chosen segment of $\partial\Omega$ one of the co-ordinates is fixed and the

other is disturbed arbitrarily but monotonically. In the (ξ, η)-plane the domain Ω will be represented by the rectangle Ω_T. Consider the transformation

$$\xi = \xi(x, y), \qquad \eta = \eta(x, y), \qquad \tau = t \tag{7}$$

with the Jacobian $J = x_\xi y_\eta - x_\eta y_\xi$, $0 \neq J < \infty$. In the new variables equations (1) and (2) transform

$$U_t + \frac{(U^2/H)_\xi y_\eta - (U^2/H)_\eta y_\xi + (UV/H)_\eta x_\xi - (UV/H)_\xi x_\eta}{J} + \frac{gH(\zeta_\xi y_\eta - \zeta_\eta y_\xi)}{J}$$

$$= fV + k_w w_{(x)}|\mathbf{w}| - \mu \frac{U|\mathbf{V}|}{H^2} + \mu_1 \nabla^2_{\xi,\eta} U - \frac{H}{\rho_0 J}\left(\frac{\partial p_a}{\partial \xi} y_\eta - \frac{\partial p_a}{\partial \eta} y_\xi\right), \tag{8}$$

$$V_t + \frac{(V^2/H)_\eta x_\xi - (V^2/H)_\xi x_\eta + (UV/H)_\xi y_\eta - (UV/H)_\eta y_\xi}{J} + \frac{gH(\zeta_\eta x_\xi - \zeta_\xi x_\eta)}{J}$$

$$= -fU + k_w w_{(y)}|\mathbf{w}| - \mu \frac{V|\mathbf{V}|}{H^2} + \mu_1 \nabla^2_{\xi,\eta} V - \frac{H}{\rho_0 J}\left(\frac{\partial p_a}{\partial \eta} x_\xi - \frac{\partial p_a}{\partial \xi} x_\eta\right). \tag{9}$$

Multiplying equation (8) by $J^{-1} y_\eta$, equation (9) by $-J^{-1} x_\eta$ and summing them, we obtain equation (10) in which the main terms are expressed via the contravariant fluxes. Similarly, multiplying equation (8) by $-J^{-1} y_\xi$, equation (9) by $J^{-1} x_\xi$ and summing them, we get equation (11). Equations (1)–(3) assume the form

$$P_t + \frac{gH}{J}(g_{22}\zeta_\xi - g_{12}\zeta_\eta) = -J^{-1}(\mathscr{A} y_\eta - \mathscr{B} x_\eta) + f\tilde{Q} + k_w|\mathbf{w}|(w_{(x)} y_\eta - w_{(y)} x_\eta) - \mu \frac{P|\mathbf{V}|}{H^2}$$

$$+ \mu_1(\nabla^2 U y_\eta - \nabla^2 V x_\eta) - \frac{H}{\rho_0 J}\left(\frac{\partial p_a}{\partial \xi} g_{22} - \frac{\partial p_a}{\partial \eta} g_{12}\right) \equiv \Psi_1, \tag{10}$$

$$Q_t + \frac{gH}{J}(g_{11}\zeta_\eta - g_{12}\zeta_\xi) = -J^{-1}(\mathscr{A} x_\xi - \mathscr{B} y_\xi) - f\tilde{P} + k_w|\mathbf{w}|(w_{(y)} x_\xi - w_{(x)} y_\xi) - \mu \frac{Q|\mathbf{V}|}{H^2}$$

$$+ \mu_1(\nabla^2 V x_\xi - \nabla^2 U y_\xi) - \frac{H}{\rho_0 J}\left(\frac{\partial p_a}{\partial \eta} g_{11} - \frac{\partial p_a}{\partial \xi} g_{12}\right) \equiv \Psi_2, \tag{11}$$

$$\zeta_t + J^{-1}(P_\xi + Q_\eta) = \omega_s, \tag{12}$$

where $P = Uy_\eta - Vx_\eta$ and $Q = Vx_\xi - Uy_\xi$ are the contravariant components of flux, $\mathscr{A} = (PUH^{-1})_\xi + (QUH^{-1})_\eta$, $\mathscr{B} = (QVH^{-1})\eta + (PVH^{-1})_\xi$, $g_{11} = x_\xi^2 + y_\xi^2$, $g_{22} = x_\eta^2 + y_\eta^2$ and $g_{12} = x_\xi x_\eta + y_\eta y_\xi$ are the covariant components of the metric tensor, $\tilde{P} y_\xi = J^{-1}(g_{11}P + g_{12}Q) = Ux_\xi + V_{y\xi}$ and $\tilde{Q} = J^{-1}(g_{22}Q + g_{12}P) = Vy_\eta + Ux_\eta$ are the covariant components of flux and $|\mathbf{V}| = (U^2 + V^2)^{1/2} = [(P\tilde{P} + Q\tilde{Q})/J]^{1/2}$. The Cartesian components of flux U and V can be expressed via the contravariant fluxes P and Q as

$$U = (Px_\xi + Qx_\eta)/J, \qquad V = (Qy_\eta + Py_\xi)/J. \tag{13}$$

Laplacians in curvilinear co-ordinates may be expressed as

$$\nabla^2 \phi = J^{-2}(g_{22}\phi_{\xi\xi} + g_{11}\phi_{\eta\eta} - 2g_{12}\phi_{\xi\eta}) + (\xi_{xx} + \xi_{yy})\phi_\xi + (\eta_{xx} + \eta_{yy})\phi_\eta. \tag{14}$$

If the curvilinear grid is generated with the elliptical method,[7] then the last two terms in equation

(14) are equal to zero and the expressions for the lateral eddy viscosity terms in (10) and (11) may be simplified to

$$\mu_l(\nabla^2 U y_\eta - \nabla^2 V x_\eta) \approx \frac{\mu_l}{J^2}(g_{22}P_{\xi\xi} + g_{11}P_{\eta\eta}), \qquad \mu_l(\nabla^2 V x_\xi - \nabla^2 U y_\xi) \approx \frac{\mu_l}{J^2}(g_{11}Q_{\eta\eta} + g_{22}Q_{\xi\xi}).$$

Finally the system (10)–(12) can be written in a matrix form as

$$\mathbf{W}_t + A\mathbf{W}_\xi + B\mathbf{W}_\eta = \Psi, \quad \xi, \eta \in \Omega_T, \quad t \geq 0, \tag{15}$$

where

$$\mathbf{W} = \begin{pmatrix} P \\ Q \\ \zeta \end{pmatrix}, \qquad A = \begin{pmatrix} 0 & 0 & gHJ^{-1}g_{22} \\ 0 & 0 & -gHJ^{-1}g_{12} \\ J^{-1} & 0 & 0 \end{pmatrix},$$

$$B = \begin{pmatrix} 0 & 0 & -gHJ^{-1}g_{12} \\ 0 & 0 & gHJ^{-1}g_{11} \\ 0 & J^{-1} & 0 \end{pmatrix}, \qquad \Psi = \begin{pmatrix} \Psi_1 \\ \Psi_2 \\ \omega_s \end{pmatrix}.$$

Boundary problem formulation

Let us consider the formulation of boundary conditions in curvilinear co-ordinates (e.g. for $\xi = \text{const.}$ boundary) for the hyperbolic case $\mu_l \to 0$. The system (8), (9), (12) can be written in the form

$$\mathbf{u}_t + \hat{A}\mathbf{u}_\xi + \hat{B}\mathbf{u}_\eta = \hat{\Psi}, \quad \xi, \eta \in \Omega_T, \quad t \geq 0, \tag{16}$$

where

$$\mathbf{u} = \begin{pmatrix} U/H \\ V/H \\ \zeta \end{pmatrix}, \qquad \hat{A} = \begin{pmatrix} P/JH & 0 & g\xi_x \\ 0 & P/JH & g\xi_y \\ H\xi_x & H\xi_y & P/JH \end{pmatrix}, \qquad \hat{B} = \begin{pmatrix} Q/JH & 0 & g\eta_x \\ 0 & Q/JH & g\eta_y \\ H\eta_x & H\eta_y & Q/JH \end{pmatrix}.$$

To diagonalize the matrix $\hat{A}$, we introduce the matrix S^{-1} whose strings are eivenvectors of $\hat{A}$:

$$S^{-1} = \begin{pmatrix} -b & a & 0 \\ a/\sqrt{2} & b/\sqrt{2} & \sqrt{(2g/H)} \\ a/\sqrt{2} & b/\sqrt{2} & \sqrt{(2g/H)} \end{pmatrix}.$$

After the transformation $\Lambda = S^{-1}\hat{A}S$ the matrix A converts to diagonal form:

$$\Lambda = \begin{pmatrix} PJ^{-1}H^{-1} & 0 & 0 \\ 0 & (PH^{-1} + s_p)J^{-1} & 0 \\ 0 & 0 & (PH^{-1} - s_p)J^{-1} \end{pmatrix},$$

where $s_p = \sqrt{(gH\, g_{22})}$.

Multiplying equation (16) by S^{-1}, we obtain

$$\omega_t + \Lambda\omega_\xi = \mathbf{F}, \qquad \omega = S^{-1}\mathbf{u} = (\omega_0, \omega_+, \omega_-),$$

$$\omega_0 = \frac{1}{H}(-bU + aV) = -\frac{\tilde{Q}}{H\sqrt{g_{22}}}, \qquad \omega_\pm = \frac{1}{\sqrt{2}}\left[\frac{P}{H\sqrt{g_{22}}} \pm \sqrt{\left(\frac{g}{H}\right)}\zeta\right],$$

where the right-hand side **F** does not influence the behaviour of the characteristic matrix on $\partial\Omega_1^*$. Thus the transfer to curvilear co-ordinates changes the tangential velocity component of the covariant one and the normal velocity component of the contravariant one.

For $0 < P < s_p H$ the matrix Λ on $\partial\Omega_1^*$ has two positive eigenvalues, i.e. two boundary conditions should be implied for the inflow. For $P < 0$ the matrix Λ has only one positive eigenvalue, so one boundary condition should be implied for the outflow. In accordance with (5) and (6), the boundary conditions for the hyperbolic case ($\mu_1 = 0$) have the form

$$\begin{aligned} P + s_p\zeta &= \gamma_1, \quad \text{and} \quad \tilde{Q} = \gamma_2 \quad \text{on the inflow } \xi = \text{const. boundary,} \\ Q + s_q\zeta &= \gamma_3, \quad \text{and} \quad \tilde{P} = \gamma_4 \quad \text{on the inflow } \eta = \text{const. boundary,} \end{aligned} \tag{17}$$

$$\begin{aligned} P - s_p\zeta &= \gamma_5 \quad \text{on the outflow } \eta = \text{const. boundary,} \\ Q - s_q\zeta &= \gamma_6 \quad \text{on the outflow } \eta = \text{const. boundary,} \end{aligned} \tag{18}$$

where $s_q = \sqrt{(ghg_{11})}$. The homogeneous forms of (18) is often used as the condition which allows a wave to leave an area of computation ('free exit' condition). In Cartesian co-ordinates it has the form of a relation between the normal component of velocity and surface elevation:

$$v_n = \pm\sqrt{(g/h)}\zeta.$$

In curvilinear co-ordinates for the lines $\xi = \text{const.}$ we have

$$P = \pm s_p\zeta \tag{19}$$

and for the lines $\eta = \text{const.}$

$$Q = \pm s_q\zeta. \tag{20}$$

On the solid parts of the boundary $\partial\Omega_1^*$ the condition $v_n = 0$ transfers to $v_n = \mathbf{v}\cdot\nabla\xi^i = 0$, $i = 1, 2$, i.e.

$$\begin{aligned} P &= 0 \quad \text{on } \xi = \text{const.}, \\ Q &= 0 \quad \text{on } \eta = \text{const.} \end{aligned} \tag{21}$$

In accordance with (4)–(6), conditions (17), (18) and (21) on the $\xi = \text{const.}$ boundary for the viscous shallow water equations should be augmented with the terms $\mu_1\partial(g_{22}^{-1/2}P)\partial n$ and $\mu_1\partial(g_{11}^{-1/2}Q)\partial n$. Here $\partial/\partial n$ is the operator of the normal derivative to the line $\xi = \text{const.}$:

$$\frac{\partial}{\partial n} = \frac{1}{J\sqrt{g_{22}}}\left(g_{22}\frac{\partial}{\partial\xi} - g_{12}\frac{\partial}{\partial\eta}\right).$$

Condition (21) with $J > 0$ leads to the no-slip condition on the solid boundary $U = V = 0$.

Energy equation

In the set of equations (1)–(3) we multiply the equation of motion by **V** and the equation of continuity by $|\mathbf{V}|^2, 2H^2) + g\zeta$. After summing them and integrating over the domain Ω, we have the equation for the total energy **E**:

$$\frac{\partial\mathbf{E}}{\partial t} + \frac{1}{2}\int_{\partial\Omega}\left(\frac{U^2+V^2}{H^2} + 2g\zeta\right)\mathbf{V}_n\,\mathrm{d}s = \iint_\Omega\left[k_w|\mathbf{w}|\mathbf{w}\cdot\left(\frac{\mathbf{V}}{H}\right) - \mu\left(\frac{|\mathbf{V}|}{H}\right)^3 + \mu_1\mathbf{V}\cdot\nabla^2\left(\frac{\mathbf{V}}{H}\right)\right]\mathrm{d}x\,\mathrm{d}y,$$

$$\mathbf{E} = \frac{1}{2}\iint_\Omega\left(\frac{U^2+V^2}{H} + g\zeta^2\right)\mathrm{d}x\,\mathrm{d}y. \tag{22}$$

This equation shows that a change in energy is determined by the fluxes across open boundaries, the work of wind stresses, energy dissipation due to bottom friction and turbulent diffusion. To obtain the energy equation in curvilinear co-ordinates, we multiply the first equation of the set (15) by $\tilde{P}$, the second by $\tilde{Q}$ and the third by $g\zeta + |\mathbf{V}|^2/2H^2$. Adding the results, integrating over the domain Ω_T and using the Green formula, we have

$$\frac{\partial \mathbf{E}}{\partial t} + \frac{1}{2}\int_{\partial\Omega_T}\left[(\tfrac{1}{2}|\mathbf{V}| + g\zeta)P_n - \frac{\mu_1}{JH}\left(\tilde{P}\frac{\partial P}{\partial n} + \tilde{Q}\frac{\partial Q}{\partial n}\right)\right]ds$$
$$= \iint_{\Omega_T}\left\{k_w|\mathbf{w}|\mathbf{w}\cdot\left(\frac{\mathbf{V}}{H}\right) - \mu\left(\frac{|\mathbf{V}|}{H}\right)^2 - \mu_1\left[\nabla P\cdot\nabla\left(\frac{J^{-2}\tilde{P}}{H}\right) + \nabla Q\cdot\nabla\left(\frac{J^{-2}\tilde{Q}}{H}\right)\right]\right\}J\,d\xi\,d\eta, \quad (23)$$

where $P_n = P$ for the lines $\xi = \text{const.}$ and $P_n = Q$ for the lines $\eta = \text{const.}$

3. SEMI-IMPLICIT SCHEME FOR THE VISCOUS SHALLOW WATER EQUATIONS

Let us simplify the algorithm approximating the advection terms explicitly, though level gradient approximating implicitly. We will approximate implicitly also the bottom friction terms and explicitly the Coriolis terms and lateral eddy viscosity terms.

Factorizing the equation set (15), we obtain

$$\left(E + \frac{\Delta t}{2}A\partial_\xi\right)\left(E + \frac{\Delta t}{2}B\partial_\eta\right)\mathbf{W}^{n+1} = \left(E - \frac{\Delta t}{2}A\partial_\xi\right)\left(E - \frac{\Delta t}{2}B\partial_\eta\right)\mathbf{W}^n + \Delta t\Psi^n, \quad (24)$$

where E is the unity matrix, n is the time step number and Δt is the time step. Approximating the differential operators by the central second-order differences $\partial_\xi \sim \delta_\xi$ and $\partial_\eta \sim \delta_\eta$, we get the Crank–Nicholson scheme which can be realized by the splitting

$$\begin{aligned}\left(E + \frac{\Delta t}{2}A\delta_\xi\right)\mathbf{W}^* &= \left(E - \frac{\Delta t}{2}B\delta_\eta\right)\mathbf{W}^n + \Psi^n\frac{\Delta t}{2},\\ \left(E + \frac{\Delta t}{2}B\delta_\eta\right)\mathbf{W}^{n+1} &= \left(E - \frac{\Delta t}{2}A\delta_\xi\right)\mathbf{W}^* + \Psi^*\frac{\Delta t}{2}.\end{aligned} \quad (25)$$

Let us check the approximation of the non-uniform factorized equation (24) by the scheme (25). Excluding $\mathbf{W}^*$ from (25), we obtain

$$\frac{\mathbf{W}^{n+1} - \mathbf{W}^n}{\Delta t} + \tfrac{1}{2}A\delta_\xi(\mathbf{W}^{n+1} + \mathbf{W}^n) + \tfrac{1}{2}B\delta_\eta(\mathbf{W}^{n+1} + \mathbf{W}^n) = \tfrac{1}{2}(\Psi^n + \Psi^*) + \mathbf{R}, \quad (26)$$

where $\mathbf{R}$ is the approximation error given by

$$\mathbf{R} = -\frac{\Delta t^2}{4}A\delta_\xi(B\delta_\eta\mathbf{W}_t) + \frac{\Delta t^2}{8}A\delta_\xi\Psi_t = O(\Delta t^2).$$

Analysis of the stability of the scheme (25) for the linear case with advection neglected gives for the eigenvalues λ_i of the matrix $\frac{1}{2}(A\delta_\xi + B\delta_\eta)$

$$\lambda_1 = 0, \qquad \lambda_{2,3} = \pm i\frac{\kappa}{2}J^{-1}a,$$

where $\kappa = \Delta t/\Delta$, $a = (g_{11}\sin^2\theta_2 + g_{22}\sin^2\theta_1 - 2g_{12}\sin\theta_1\sin\theta_2)^{1/2} \geq 0$, $\theta_1 = s_1\Delta$, $\theta_2 = s_2\Delta$, s_1 and

s_2 are the grid wave numbers and $\Delta = \Delta\xi = \Delta\eta$ is the space step. The eigenvalues g_i of the transition matrix $\hat{G}$ of the scheme (26) are $g_i = (1 - \lambda_i)/(1 + \lambda_i)$, $g_1 = 1$, $|g_{2,3}| = 1$, i.e. the scheme is absolutely stable. For the general case consideration of the eigenvalues of the matrices A and B gives the following limitations on the fluxes and time step:

$$\frac{1}{H}(P, Q) \leq \sqrt{(gH)}(\sqrt{g_{22}}, \sqrt{g_{11}}), \tag{27}$$

$$\Delta t \leq \frac{JH}{\min(|P| + |Q|)}. \tag{28}$$

To estimate the phase error of the Crank–Nicholson approximation in curvilinear coordinates, let us consider two-dimensional advection with velocity (u_0, v_0). In this case $A = u_0 E$ and $B = v_0 E$ in (26) and we have

$$\hat{G} = \frac{1 - i\chi}{1 + i\chi}, \tag{29}$$

where

$$\chi = \frac{\kappa}{2}(U_0 \sin\theta_1 + V_0 \sin\theta_2), \qquad U_0 = J^{-1}(u_0 y_\eta - v_0 x_\eta), \qquad V_0 = J^{-1}(-u_0 y_\xi + v_0 x_\xi).$$

The phase shift has the form

$$\hat{\psi} = \arg(\hat{G}) = -\tan^{-1}\left(\frac{\kappa(U_0 \sin\theta_1 + V_0 \sin\theta_2)}{1 - (\kappa^2/4)(U_0 \sin\theta_1 + V_0 \sin\theta_2)^2}\right). \tag{30}$$

For fixed CFL numbers κU_0 and κV_0 the phase error increases with increasing θ. The dispersion error $1 - \hat{\psi}/\psi_0$ (where ψ_0 is the harmonic solution) decreases rapidly with decreasing θ, so the type of dispersion is normal.

Numerical realization

The structure of the matrix A permits one to exclude ζ^* from the first and third equations for $\mathbf{W}^*$ and to obtain an equation for P^* which can be solved by a tridiagonal solver. The unknowns ζ^* and Q^* can then be determined explicitly. Similarly, excluding ζ^{n+1} from the first and third equations for $\mathbf{W}^{n+1}$, we arrive at a boundary value problem with respect to Q^{n+1} which can be solved also by a tridiagonal solver and then ζ^{n+1} and P^{n+1} are found explicitly.

For the first-half step we have

$$P^* + \frac{\Delta t}{2J} gHg_{22}\delta_\xi \zeta^* = P^n + \frac{\Delta t}{2J} gHg_{12}\delta_\eta \zeta^n + \frac{\Delta t}{2}\Psi_1^n, \tag{31}$$

$$Q^* - \frac{\Delta t}{2J} gHg_{12}\delta_\xi \zeta^* = Q^n - \frac{\Delta t}{2J} gHg_{11}\delta_\eta \zeta^n + \frac{\Delta t}{2}\Psi_2^n, \tag{32}$$

$$\xi^* + \frac{\Delta t}{2J}\delta_\xi P^* = \xi^n - \frac{\Delta t}{2J}\delta_\eta Q^n + \frac{\Delta t}{2}\omega_s. \tag{33}$$

Differentiating (33) with respect to ξ and substituting the obtained expression in (31), we exclude the unknown ζ^*:

$$-P^* + \frac{\Delta t^2}{4J} gHg_{22}\delta_\xi(J^{-1}\delta_\xi P^*) - \frac{\Delta t}{2}\mu\left|\frac{P^*V^n}{H^2}\right|$$
$$= -P^n + \frac{\Delta t}{2J} gHg_{22}\delta_\xi\zeta^n - \frac{\Delta t}{2J} gHg_{12}\delta_\eta\zeta^n - \frac{\Delta t^2}{4J} gHg_{22}\delta_\xi(J^{-1}\delta_\eta Q^n) - \frac{\Delta t}{2}\Psi_1^n. \quad (34)$$

The non-linear bottom friction term is linearized and approximated implicitly. Equation (34) with two conditions for P^* on opposite boundaries can be solved by a tridiagonal solver. Then we can find the unknowns ζ^* and Q^* explicitly from (32) and (33). The second half-step is similar.

It is convenient to use the space-staggered C grid of Mesinger and Arakawa[23] with points $\xi_i\eta_j \in \Omega_\Delta$, $i = 1, 2, \ldots, l$, $j = 1, 2, \ldots, m$, in which ζ-values are defined at even grid points, P-values are defined for even-i and odd-j points and Q values for odd-i and even-j points. The depth values h may be specified at odd points.

On the solid parts of the boundary the condition of zero normal flux in the contravariant variables is very simple (21):

$$P = 0 \quad \text{on } \xi = \text{const.},$$
$$Q = 0 \quad \text{on } \eta = \text{const.}$$

On the open parts of the boundary it is very simple to assign discharges, which is often done in practical applications because they are P and Q themselves.

If the surface elevation is specified on the boundary, then from equation (33) we get the following boundary condition for equation (34):

$$\delta_\xi P^* = -J(\zeta^* - \zeta^n)/(\Delta t/2) - \delta_\eta Q^n. \quad (35)$$

With accuracy ($O(\Delta t^2)$) we may obtain $\zeta^* = \zeta(t^n + \Delta t/2)$.

The third type of open boundary is the 'free exit' one through which disturbances may leave an area of computation, equations (19) and (20). To obtain the 'free exit' boundary condition for equation (34), we exclude ζ^* from (34) and (19) and for the ξ = const. boundary we then have

$$P_i^* = \frac{1}{1 + (s_F s)^{-1}} P_{i\pm 2}^* + \frac{\mp\zeta_{i\pm 1}^n \pm s(Q_{j+1}^n - Q_{j-1}^n)_{i\pm 1}}{s_p^{-1} + s}. \quad (36)$$

For the η = const. boundary this condition has the form

$$Q_j^{n+1} = \frac{1}{1 + (s_q s)^{-1}} Q_{j\pm 2}^{n+1} + \frac{\mp\zeta_{j\pm 1}^* \pm s(P_{i+1}^* - P_{i-1}^*)_{j\pm 1}}{s_q^{-1} + s}, \quad (37)$$

where $s = \Delta t(2J)^{-1}$.

To approximate the derivative $\delta_\eta\zeta^n$ in equation (34) near the η = const. boundary at P-points, we must use one-sided differences including four nearby ζ-points instead of central ones. The same procedure is adopted when solving equation (32). The stability of this procedure for the Crank–Nicholson scheme was shown by Abarbanel and Murman[24] based on the approach developed by Gustaffson *et al.*[25]

The approximation of lateral eddy diffusion terms near solid boundaries requires the assignment of values of a flux P_{-1}, Q_{-1} at points which lie outside the grid. The assignment of zero values may lead to a significant error in velocity cross-section profiles, because the grid

refinement is usually not perfect. We adopt a quadratic friction law condition analogous to the bottom friction one:

$$\mu_l \frac{\partial U}{\partial n} = l_w \frac{U|\mathbf{V}|}{H} \quad (\eta = \text{const.}), \qquad \mu_l \frac{\partial V}{\partial n} = l_w \frac{V|\mathbf{V}|}{H} \quad (\xi = \text{const.}), \tag{38}$$

where l_w is an empirical wall friction coefficient. Turning to curvilinear co-ordinates, we can obtain after linearization and some simplifications

$$P_{-1} = P_1 \Big/ \left(1 + \frac{l_w J}{\mu_l H \sqrt{g_{11}}} |\mathbf{V}|\right), \qquad Q_{-1} = Q_1 \Big/ \left(1 + \frac{l_w J}{\mu_l H \sqrt{g_{22}}} |\mathbf{V}|\right). \tag{39}$$

Testing

Figure 1 shows an example of the computation of free oscillations in a circle mapped on to a rectangle using this algorithm with zero advection and friction. In a zone of the refined computational grid the CFL number reaches a value $O(10^2)$. The first mode of oscillations at the circle centre is compared with the analytical solution[26] $\zeta(r, t) = \zeta_0 J_0(kr) \cos(\omega t)$, where J_0 is a zero-order Bessel function, $k = 1{\cdot}21979\pi/R$, $\omega = k\sqrt{(gh)}$ and R is the radius of the basin. The wave height practically coincides with the analytical solution, while the wave frequency is somewhat slower than the analytical one. Upon decreasing the time step, the phase velocity error becomes smaller.

Another test was the computation of a large vortex in a channel with a sudden expansion of its width. the result was compared with hydraulic model data obtained by G. V. Stefanofich at the B. E. Vedeneev Hydrotechnical Institute in St. Petersburg especially for the testing of numerical models. The water depth was 10 cm, the discharge 0·052 $m^3\ s^{-1}$ and the Mannings number $n = 0{\cdot}0136$. The computational grid consisted of 51 × 53 points and Δt was taken equal to 0·01 s. The vortex is a result of non-linear advection and lateral eddy viscosity. The current in the hydraulic model displayed a slightly oscillating behaviour and the average length of the vortex zone was approximately 5·3 m. In computations we found a vortex length equal to 4·6 m (Figure 2). The length increases with decreasing lateral eddy coefficient μ_l, but at smaller values of μ_l the velocity field starts to oscillate. We should note that in this experiment the transport of turbulent energy was significant and more precise results can only be obtained by taking this factor into consideration. For μ_l we used the expression $\mu_l = kL^2(u_y^2 + v_x^2)^{1/2}$, where k is an empirical coefficient and L is the local grid spacing. Turning to curvilinear co-ordinates and omitting the second-order terms, we have

$$\mu_l = \frac{kL^2}{J^2 H} [P_\eta^2(x_\xi^4 + y_\xi^4) + Q_\xi^2(y_\eta^4 + x_\eta^4)]^{1/2}.$$

The best result for the length of the vortex zone was obtained with $k = 0{\cdot}015$. However, for real size objects this value was found to be too small. The value of the wall friction coefficient l_w according to this experiment and also to a comparison with field data for the Amur river (see Section 6) lies in the range 0·02–0·7.

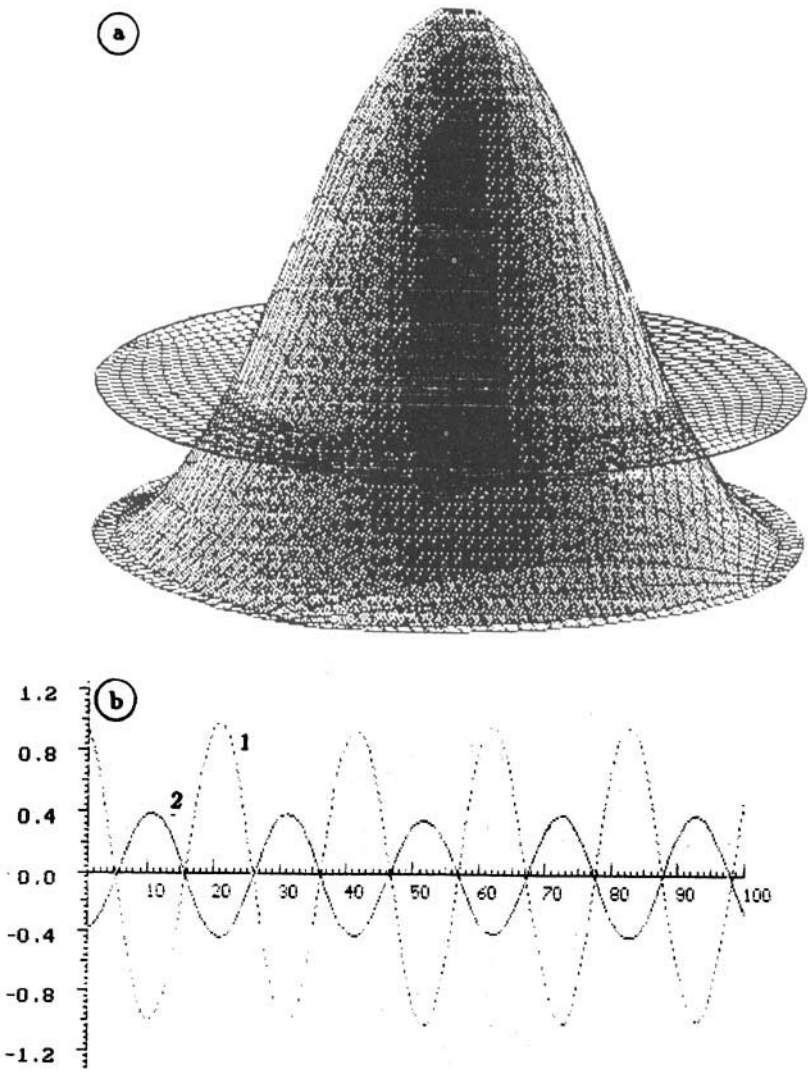

Figure 1. Analytical testing of semi-implicit scheme. (a) Initial surface level for zero-order Bessel function in a circular cylindrical basin. Boundary walls are not shown. (b) Level oscillations in centre (1) and near a wall (2). Analytical period of oscillation is equal to 20 time steps

4. ADVECTION–DIFFUSION EQUATION IN CURVILINEAR CO-ORDINATES

In the domain Q_2 the depth-averaged contaminant cocentration field evolution can be described by

$$(cH)_t + (Uc)_x + (Vc)_y = \mu_c \nabla^2(cH) - \lambda cH + \omega_s c_s, \tag{40}$$

an equation which is obtained by vertical integration of the three-dimensional equation with the condition $\partial c/\partial n|_{\partial\Omega} = 0$ and kinematic conditions on the free surface and at the bottom. Here c is the concentration of pollutant, μ_c is the diffusion coefficient, λ is the coefficient of

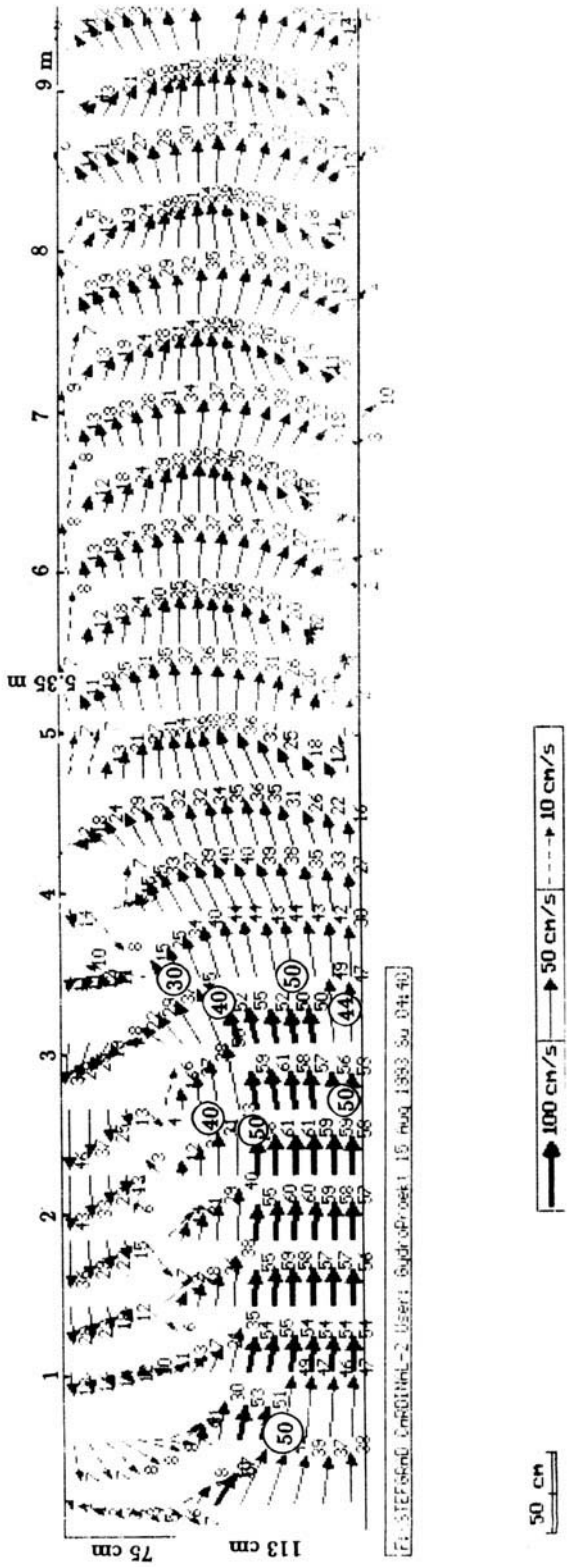

Figure 2. Flow in a channel with sudden expansion of its width. Numerical model and hydraulic model (digits in circles) results. Discharge 0·052 $m^3 s^{-1}$, depth $h = 10{\cdot}1$ cm, time step $\Delta t = 0{\cdot}001$ s grid 53 × 51, Mannings number $n = 0{\cdot}0136$, lateral viscosity $\mu_1 = 0{\cdot}015L^2\sqrt{(u_y^2 + v_x^2)}$

non-conservativity and c_s is the source concentration. Note that in the derivation of this equation it is assumed, besides the assumption conforming to the shallow water theory, i.e.

$$\int_{-h}^{\zeta} \tilde{c}(x, y, z, t)\tilde{v}(x, y, z, t)\,dz = H^{-1}\int_{-h}^{\zeta} \tilde{c}(x, y, z, t)\,dz \int_{-h}^{\zeta} \tilde{v}(x, y, z, t)\,dz,$$

that the terms $\nabla(c|_{\zeta}\cdot\nabla\zeta)$ and $\nabla(c|_{-h}\cdot\nabla h)$ are small. It is valid for non-abrupt changes in depths and water surface. This equation is solved under a boundary condition of the type

$$k_1 c + \mu_c \frac{\partial c}{\partial n}\bigg|_{\partial\Omega} = \psi \tag{41}$$

and some initial condition.

One of the difficulties in solving the advection–diffusion equation is to approximate correctly the advection terms. The appropriate scheme should be accurate enough and possess acceptable dissipative and dispersive properties. Preferred schemes for describing the advection are based on approximations using directed or biased–directed finite differences that correspond to the hyperbolic character of the problem in the case where advection prevails. For such processes, when the Peclet grid number $P = |\mathbf{v}|\Delta/\mu_c \gg 1$, the time step for explicit schemes is determined by the CFL criterion $\Delta t \sim |\mathbf{v}|^{-1}\Delta$. In zones of small-scale geometry Δt can be rather small. Thus an implicit method of integration of the equation is preferable. The use of directed or biased–directed finite differences improves the dispersive properties of the scheme as compared with the central finite difference approximation of advection, controls the scheme's viscosity and facilitates the boundary condition formulation if the diffusion is negligible. One way to attain an accuracy higher than second-order is to use compact finite differences which conserve a three-point stencil.[27] Below, a scheme of accuracy $O(\Delta^3, \Delta t^2)$ is implemented by a pentadiagonal solver along the co-ordinates.

We make use of the transformation $\xi = \xi(x, y)$, $\eta = \eta(x, y)$, which is consistent with the configuration $\Omega(x, y)$. Using the contravariant fluxes P and Q, we can readily rewrite the advection terms in curvilinear co-ordinates using the mass conservation law as

$$(Uc)_x + (Vc)_y = \frac{1}{J}[(Pc)_\xi + (Qc)_\eta]. \tag{42}$$

The exact expression for the diffusion terms is obtained after some transformations as

$$\mu_c\nabla^2(cH) = \mu_c[(g_{22}HJ^{-1}c_\xi)_\xi + (g_{11}HJ^{-1}c_\eta)_\eta - (g_{12}HJ^{-1}c_\eta)_\xi - (g_{12}HJ^{-1}c_\xi)_\eta]. \tag{43}$$

Although this is a conservative form, it would be difficult to use this expression because it contains derivatives of the Jacobian and of the metric coefficients. As mentioned above for the elliptical grid, a simpler formula may be obtained:

$$\mu_c\nabla^2(cH) = \frac{\mu_c H}{J}(g_{22}c_{\xi\xi} + g_{11}c_{\eta\eta} - 2g_{12}c_{\xi\eta}). \tag{44}$$

Thus in curvilinear co-ordinates the advection–diffusion equation has the form

$$J(Hc)_t + (Pc)_\xi + (Qc)_\eta = \frac{\mu_c H}{J}(g_{22}c_{\xi\xi} + g_{11}c_{\eta\eta} - 2g_{12}c_{\xi\eta}) - \lambda JHc + w_s c_s, \tag{45}$$

where $w_s = J\omega_s$ is the source discharge.

5. HYBRID SCHEME FOR ADVECTION–DIFFUSION EQUATION

To solve equation (45), let us use the splitting

$$\frac{J}{\Delta t/2}[(Hc)^* - (Hc)^n] + \delta_\xi(Pc)^* + \delta_\eta(Qc)^n - \frac{\mu_c H^n}{J}(g_{22}\delta_{\xi\xi}c^* + g_{11}\delta_{\eta\eta}c^n - 4g_{12}\delta_{\xi\eta}c^n)$$
$$= -2\lambda JHc^* + 2w_s c_s, \tag{46}$$

$$\frac{J}{\Delta t/2}[(Hc)^{n+1} - (Hc)^*] + \delta_\xi(Pc)^* + \delta_\eta(Qc)^{n+1} - \frac{\mu_c H^*}{J}(g_{22}\delta_{\xi\xi}c^* + g_{11}\delta_{\eta\eta}c^{n+1}) = 0. \tag{47}$$

We will approximate the advection terms by a hybrid of first- and third-order upwind finite differences as

$$\delta_\xi(Pc) = \frac{1}{\Delta}[\beta_R^+ F_R^+ - \beta_L^+ F_L^+ + \beta_R^- F_R^- - \beta_L^- F_L^- + (1-\beta_R^+)f_R^+ - (1-\beta_L^+)f_L^+$$
$$+ (1-\beta_R^-)f_R^- - (1-\beta_L^-)f_L^+], \tag{48}$$

where F are the third-order, right (R) or left (L), positive (+) or negative (−) pollution fluxes and f are the corresponding first-order fluxes:

$$F_R^+ = \begin{cases} (\frac{1}{3}c_{i+1} + \frac{5}{6}c_i - \frac{1}{6}c_{i-1})P_R^+ & \text{on } i \neq l-1, \\ (\frac{3}{2}c_i - \frac{1}{2}c_{i-1})P_{i+1}^+ & \text{on } i = l-1, \end{cases}$$

$$F_R^- = \begin{cases} (\frac{1}{3}c_i + \frac{5}{6}c_{i+1} - \frac{1}{6}c_{i+2})P_R^- & \text{on } i \neq l-1, \\ c_{i+1}P_{i+1}^- & \text{on } i = l-1, \end{cases}$$

$$F_L^- = \begin{cases} (\frac{1}{3}c_{i-1} + \frac{5}{6}c_i - \frac{1}{6}c_{i+1})P_L^- & \text{on } i \neq 2, \\ (\frac{3}{2}c_i - \frac{1}{2}c_{i+1})P_{i-1}^- & \text{on } i = 2, \end{cases} \qquad F_L^+ = \begin{cases} (\frac{1}{3}c_i + \frac{5}{6}c_{i-1} - \frac{1}{6}c_{i-2})P_L^+ & \text{on } i \neq 2, \\ c_{i-1}P_{i-1}^+ & \text{on } i = 2, \end{cases}$$

$$f_R^+ = c_i P_R^+, \qquad f_L^+ = c_{i-1}P_L^+, \qquad f_R^- = c_{i+1}P_R^-, \qquad f_L^- = c_i P_L^-.$$

Here

$$P_R^\pm = (P_{i+1/2} \pm |P_{i+1/2}|)/2, \qquad P_L^\pm = (P_{i-1/2} \pm |P_{i-1/2}|)/2.$$

Second-order extrapolation is used for F_R^+ on $i = l-1$ and for F_L^- on $i = 2$ in order not to include in the advection term the boundary points $i = 1$ and $i = l$ for outgoing fluxes (but these points still remain in the diffusion terms).

A weighting function β may be chosen according to

$$\beta_R^+ = \left|1 - \frac{|c_{i-1} - 2c_i + c_{i+1}|}{|c_{i+1} - c_i| + |c_i - c_{i-1}|}\right|, \qquad \beta_R^- = \left|1 - \frac{|c_{i+2} - 2c_{i+1} + c_i|}{|c_{i+1} - c_i| + |c_{i+2} - c_{i+1}|}\right| \tag{49}$$

and so on. In regions of abrupt function variability β tends to zero, so the first-order approximation will prevail and numerical dispersion will decrease. For regions of smooth concentration distribution β tends to unity and the third-order approximation will prevent scheme diffusion.

Substituting these expressions for F and f and the second-order approximation for the

diffusion terms, we obtain a hybrid approximation for the advection–diffusion equation. For the first half-step (46) we have

$$Ac_{i-2}^{*} + Bc_{i-1}^{*} + Cc_{i}^{*} + Dc_{i+1}^{*} + Ec_{i+2}^{*} = \phi^{n}, \tag{50}$$

where $A = -\beta_{\mathrm{L}}^{+}P_{\mathrm{L}}^{+}/6$ on $i \neq 2$ and $A = 0$ on $i = 2$, $E = \beta_{\mathrm{R}}^{-}P_{\mathrm{R}}^{-}/6$ on $i \neq l-1$ and $E = 0$ on $i = l-1$, $B = \mu_{\mathrm{c}}HJ^{-1}g_{22} - \bar{b}$, $D = \mu_{\mathrm{c}}HJ^{-1}g_{22} - \bar{d}$, $C = JH(-2/\Delta t + \lambda) - 2\mu_{\mathrm{c}}HJ^{-1}g_{22} - \bar{c}$ and $\phi^{n} = \delta_{\eta}(Qc)^{n} - \mu_{\mathrm{c}}HJ^{-1}(g_{11}\delta_{\eta\eta}c - 4g_{12}\delta_{\xi\eta}c)^{n} + 2/\Delta t(-JH^{n}c^{n} - \omega_{\mathrm{s}}c_{\mathrm{s}})$, with

$$\bar{b} = \begin{cases} -\beta_{\mathrm{R}}^{+}(\frac{1}{3}P_{\mathrm{L}}^{-} + \frac{1}{6}P_{\mathrm{R}}^{+}) - (1 - \frac{1}{6}\beta_{\mathrm{L}}^{+})P_{\mathrm{L}}^{+} & \text{on } 3 \leq i \leq l-2, \\ -\frac{1}{6}\beta_{\mathrm{R}}^{+}P_{\mathrm{R}}^{+} - P_{1}^{+} & \text{on } i = 2, \\ -\beta_{\mathrm{R}}^{+}(\frac{1}{3}P_{\mathrm{L}}^{-} + \frac{1}{2}P_{l}^{+}) - (1 - \frac{1}{6}\beta_{\mathrm{L}}^{+})P_{\mathrm{L}}^{+} & \text{on } i = l-1, \end{cases}$$

$$\bar{d} = \begin{cases} \beta_{\mathrm{R}}^{+}(\frac{1}{3}P_{\mathrm{R}}^{+} + \frac{1}{6}P_{\mathrm{L}}^{-}) + (1 - \frac{1}{6}\beta_{\mathrm{R}}^{-})P_{\mathrm{R}}^{-} & \text{on } 3 \leq i \leq l-2, \\ \frac{1}{6}\beta_{\mathrm{R}}^{+}P_{\mathrm{L}}^{-} + P_{l}^{-} & \text{on } i = l-1, \\ \beta_{\mathrm{R}}^{+}(\frac{1}{3}P_{\mathrm{R}}^{+} + \frac{1}{2}P_{1}^{-}) + (1 - \frac{1}{6}\beta_{\mathrm{R}}^{-})P_{\mathrm{R}}^{-} & \text{on } i = 2, \end{cases}$$

$$\bar{c} = \begin{cases} (1 - \frac{1}{6}\beta_{\mathrm{R}}^{+})(P_{\mathrm{R}}^{+} - P_{\mathrm{L}}^{-}) + \frac{1}{3}(\beta_{\mathrm{R}}^{-}P_{\mathrm{R}}^{-} - \beta_{\mathrm{L}}^{+}P_{\mathrm{L}}^{+}) & \text{on } 3 \leq i \leq l-2, \\ (1 - \frac{1}{6}\beta_{\mathrm{R}}^{+})P_{\mathrm{R}}^{+} + \frac{1}{3}\beta_{\mathrm{R}}^{-}P_{\mathrm{R}}^{-} + (-\frac{1}{2}\beta_{\mathrm{R}}^{+} - 1)P_{1}^{-} & \text{on } i = 2, \\ -(1 - \frac{1}{6}\beta_{\mathrm{R}}^{+})P_{\mathrm{L}}^{-} - \frac{1}{3}\beta_{\mathrm{L}}^{+}P_{\mathrm{L}}^{+} + (\frac{1}{2}\beta_{\mathrm{R}}^{+} + 1)P_{l}^{+} & \text{on } i = l-1. \end{cases}$$

The five unknowns c_{i-2}, c_{i-1}, $c_i c_{i+1}$ and c_{i+2} in each finite difference equation can be found using a pentadiagonal solver of the form

$$\alpha_1 = 0, \qquad \beta_1 = 0, \qquad \gamma_1 = 0,$$

$$\alpha_2 = -D_1/C_1, \qquad \beta_2 = 0, \qquad \gamma_2 = \phi_1/C_1,$$

$$\alpha_{i+1} = [-D_i - \beta_i(B_i + A_i\alpha_{i-1})]/R_i, \qquad \beta_{i+1} = -E_i/R_i,$$

$$\gamma_{i+1} = [\phi_i - B_i\gamma_i - A_i(\alpha_{i-1}\gamma_i + \gamma_{i-1})]/R_i, \quad i = 3, \ldots, l-1,$$

where $R_i = C_i + \alpha_i(A_i\alpha_{i-1} + B_i) + A_i\beta_{i-1}$ and the boundary conditions have the form $C_1c_1 + D_1c_2 = \phi_1$ and $B_lc_{l-1} + C_lc_l = \phi_l$. After finding the coefficients α, β and γ, we can obtain the concentrations

$$c_l = (\phi_l - B_l\gamma_l)/(B_l\alpha_l + C_l), \qquad c_{l-1} = \alpha_l c_l + \gamma_l,$$

$$c_i = \alpha_{i+1}c_{i+1} + \beta_{i+1}c_{i+2} + \gamma_{i+1}, \quad i = l-2, \ldots, 1.$$

It can be shown that this approximation of the advection terms satisfies the mass conservation laws:

$$\sum_{i=2}^{l-1} \delta_{\xi}(Pc)\Delta\xi = c_1P_1^{+} + |c_lP_l^{-}| - [c_2 + \tfrac{1}{2}\beta_{2,\mathrm{R}}^{+}(c_2 - c_3)]|P_1^{-}| + [c_{l-1} + \tfrac{1}{2}\beta_{l-1,\mathrm{R}}^{+}(c_{l-1} - c_{l-2})]|P_l^{+}|. \tag{51}$$

The first and second terms on the right-hand side of (51) describe the input of pollutants from the left and right boundaries respectively, while the two last terms describe the outgoing fluxes from the left and right boundaries respectively. If $\beta_{2,\mathrm{R}}^{+} = 0$, then the outgoing flux is equal to $P_1^{-}c_2$, while if $\beta_{2,\mathrm{R}}^{+} = 1$, then this flux is equal to $(3c_2/2 - c_3/2)P_1^{-}$. To obtain equation (51), it was necessary to satisfy the following restriction on the weighting function:

$$(\beta_{\mathrm{R}}^{-})_i = (\beta_{\mathrm{R}}^{+})_{i+1}, \qquad (\beta_{\mathrm{R}}^{+})_i = (\beta_{\mathrm{L}}^{+})_{i+1}.$$

Equation (49) satisfies this constraint.

In solving equation (46) and (47), we should use the value of P, Q and H defined on the intermediate time step, so we should solve the combined dynamics and advection–diffusion equations with the same time step. Only in this case will the change in pollution volume in a grid cell be balanced by the change in cell water volume.

Testing

The numerical scheme given above was tested on analytical solutions of several model problems. As a first example let us consider the problem of diffusion of contaminant in a circular basin. The initial field of contaminant has the form

$$c^0 = c_0 e^{-\varepsilon(r/R)^2}, \qquad r^2 = x^2 + y^2. \tag{52}$$

On the lateral surface of the basin where $r = R$ the condition of zero contaminant flux is set, i.e. $\partial c/\partial n = 0$. The analytical solution is given by

$$c(r, t) = \frac{2c_0}{R^2} \sum_{n=1}^{\infty} \left[e^{-\mu_c \nu_n^2 t/R^2} \frac{J_0(\nu_n r/R)}{J_0^2(\nu_n)} \int_0^R \rho e^{-\varepsilon(\rho/R)^2} J_0\left(\frac{\nu_n \rho}{R}\right) d\rho \right], \tag{53}$$

where J_0 is a Bessel function of zero argument and ν_n are the positive roots of the equation $J_0'(\nu) = 0$. Numerical integration of the problem was performed firstly on a grid composed of 23×23 points. The parameter ε was taken as 3·4539. It was found[14] that the concentration profiles practically coincide over the whole domain. Only at the boundary is a slight deviation due to the approximation of the boundary condition observed. Experiments showed that this deviation decreases with grid refinement. For the implicit scheme (46), (47) the influence of the time step Δt was tested for an instability parameter $\mu_c \Delta t/\Delta_{\min}^2$ ranging from 0·25 to 15. When the scheme is absolutely stable, an appreciable increase in Δt leads to a decrease in diffusion velocity.

The horizontal advection was tested using the rotation of a pollutant spot in a circular basin with constant angular velocity. Comparison was made with upstream first-order differences and several other schemes. We concluded that the hybrid advection scheme does not diffuse the pollutant much, while oscillations are eliminated owing to the presence of the first-order scheme (Figure 3).

6. COMPUTATIONAL EXAMPLES

The model has been applied to various seas, lakes, reservoirs and rivers. In this section we provide examples of the use of the numerical methods for modelling the circulation and transport in Neva Bay in the Eastern Gulf of Finland and in the Amur river near Khabarovsk city.

Neva Bay is a shallow sea bay with depths ranging from 3 to 5 m to the west of St. Petersburg (Figure 4). The length of the bay is 20 km and its width is 15 km. At present the bay is crossed by a dam under construction aimed at protecting the city of St. Petersburg against storm surges. The length of the dam is 25 km. There are six water-sluices and two ship openings in the dam which are 100–240 m wide. Study of the impact of the dam is a very real problem for the city. In our calculations we used a grid generated by the solution of equation (14) and represented in Figure 4. The grid steps varied from about 100 m in the ship openings and water sluices of the dam up to 2·5 km. Under these conditions, for the local CFL numbers we have $Cr \approx 10$ at $\Delta t = 2$ min. The discharges of the Neva and its arms are assigned in the open part of the contour

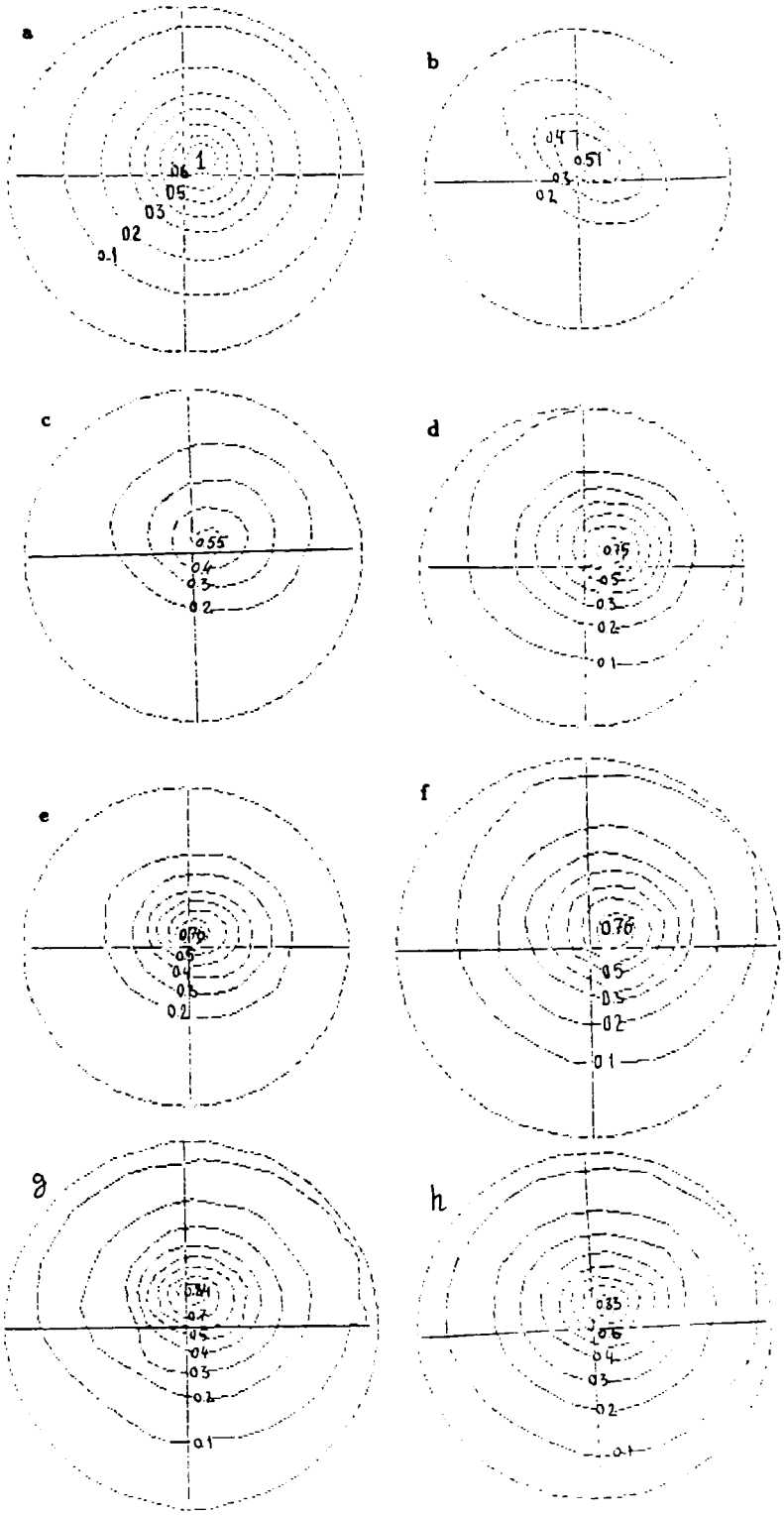

Figure 3. Computations of rotation of a pollutant spot in a circular basin. Fields of concentration after one period of rotation (50 time steps): a, initial field of concentration; b, first-order upwind scheme, Douglass–Gunn spliting; c, Jentry approximation, Peaceman–Rachford splitting; d, second-order upwind differences, Beam–Warming splitting; e, second-order central differences, Douglass–Gunn splitting; f, second-order upwind differences, Peaceman–Rachford splitting; g, second-order central differences, Peaceman–Rachford splitting; h, hybrid of first- and third-order schemes

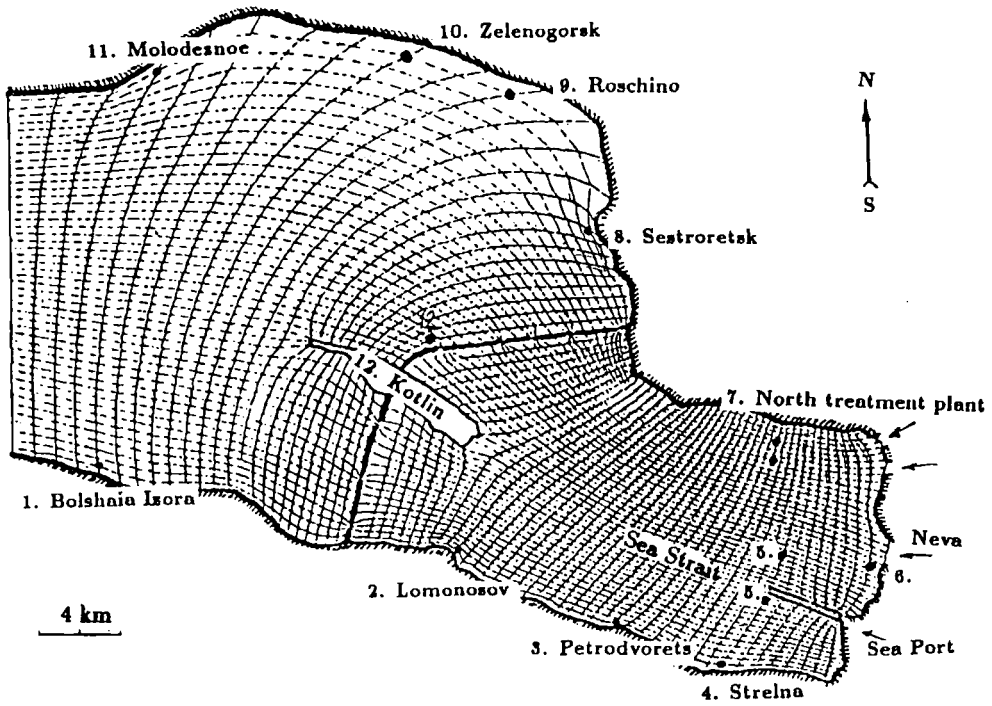

Figure 4. Curvilinear grid generated by Thompson *et al.*[7] elliptical method for Neva Bay in eastern Gulf of Finland and main treatment plant outfalls: 1, Bolshaia Izora, discharge 3×10^{10} coli-bacteria per second; 2, Lomonosov, 5×10^{10}; 3, Petrodvorets, 5×10^{10}; 4, Strelna, $6{\cdot}5 \times 10^{10}$; 5, South-west Treatment Plant, $6{\cdot}45 \times 10^{11}$; 6, Central Treatment Plants, $8{\cdot}7 \times 10^{11}$; 7, North treatment Plant, $1{\cdot}15 \times 10^{12}$; 8, Sestroretsk, 3×10^{10}; 9, Roschino, $3{\cdot}5 \times 10^{10}$; 10, Zelenogorsk, $1{\cdot}5 \times 10^{10}$; 11, Molodeznoe, $1{\cdot}4 \times 10^{10}$; 12, Kotlin, $2{\cdot}5 \times 10^{10}$

of the eastern boundary. The condition $\zeta = \zeta(t)$ is defined at the western boundary behind the dam.

Calculations of non-stationary flows in the bay under small surface level oscillations and varied meteorlogical conditions place stringent demands on a model. A rigorous test can be done by reproducing the progressive vector diagram of observed flows and the time history of surface elevation. Examples of this test are given in Figures 5 and 6. Figure 5 is a reproduction of the flow structure at a station in the south zone of the bay. We reproduce here also for comparison our previous result obtained with the three-dimensional numerical model.[14] Figure 6 is a reproduction of surface level oscillations on the south coast (Strelna) for no-dam (top) and dam (bottom) conditions. The results show that the model adequately represents the hydrodynamical regime of the bay.

Generalized estimations of the dam impact on hydrological conditions in the bay are of particular interest. Comparative analysis of the observed and computed spectra of the velocity field variability—the linear invariant of the correlation tensor—shows that the velocity vector variability under the dam conditions is markedly decreased. The results indicate that the dam is a relative barrier for high-frequency flow fluctuations with a period below 5 h, whereas waves of semidiurnal period, which predominate in the energy spectra, are essentially not distorted. The lateral turbulent eddy coefficient, which is needed in the semi-implicit scheme for smoothing, only influences relatively high-frequency oscillations. Computation of the average conditions

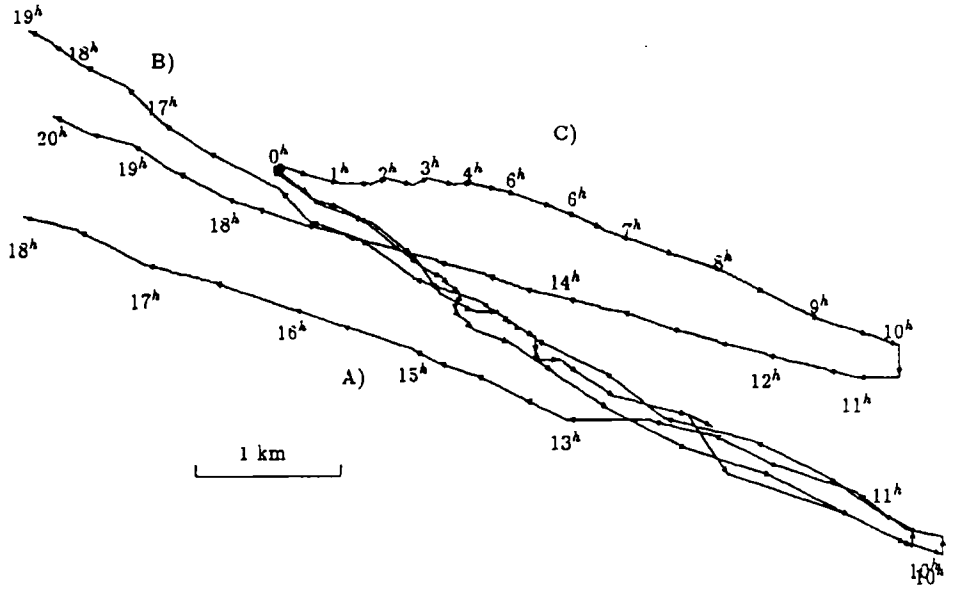

Figure 5. Progressive vector diagram of currents at a station in Neva Bay on 22 September 1981 (90 cm from bottom): A, observed; B, computed with two-dimensional model (53 × 49 grid points), $\Delta t = 6$ min; C, computed with three-dimensional model[14] (19 × 11 × 11 grid points), $\Delta t = 2$ min

over a fortnight shows that the dam decreases the western transport by less than 25%, which is about 5% of the water discharge of the Neva. Details of the numerical simulation of the Neva Bay dynamics are given in Reference 28.

The degree of pollution in Neva Bay is extremely high and the microbiological levels of pollution in the bay are catastrophic. These negative changes have been occurring over dozens of years and so it is clear that they are not entirely caused by the dam construction. The main reason is the very poor quality of treatment of waste water from St. Petersburg. The second reason is the increasing loading of pollutants from Ladoga Lake. Local outfalls of industrial waste water are large sources of pollution. It was decided to concentrate all urban and industrial wastes at three large treatment plants: the North Treatment Plant (NTP), the south-west one (SWTP) and the Central one (CTP). The choice of sites for these outfalls is strongly restricted by the presence of numerous resorts along the coast and by Kotlin Island.

The model was used to predict coliform bacteria concentrations in Neva Bay from water discharges of combined urban and industrial outfalls. The locations of the 12 most important treatment plant outfalls from St. Petersburg and its suburbs are shown on Figure 4. Their prognostic coli-bacteria discharges were determined by multiplying the projected volumes of waste water discharges for the years 1995–2000 and the forecasting concentration of coli-bacteria after treatment (5×10^6 l^{-1}). The coefficient of diffusion μ_c was taken equal to $2\ m^2\ s^{-1}$ according to measurements. Three different model runs were performed: (a, b) the main outfalls located as suggested now for (a) dam conditions and (b) natural conditions; (c) the NTP outfalls transferred 1 km offshore (2 km from the shore), the SWTP outfalls transferred 2 km to the north from the Sea Strait, dam conditions. The last example corresponds to steady state dynamics with zero surface level on the western boundary.

Figure 7 shows the concentration fields for these three cases when the steady state is reached

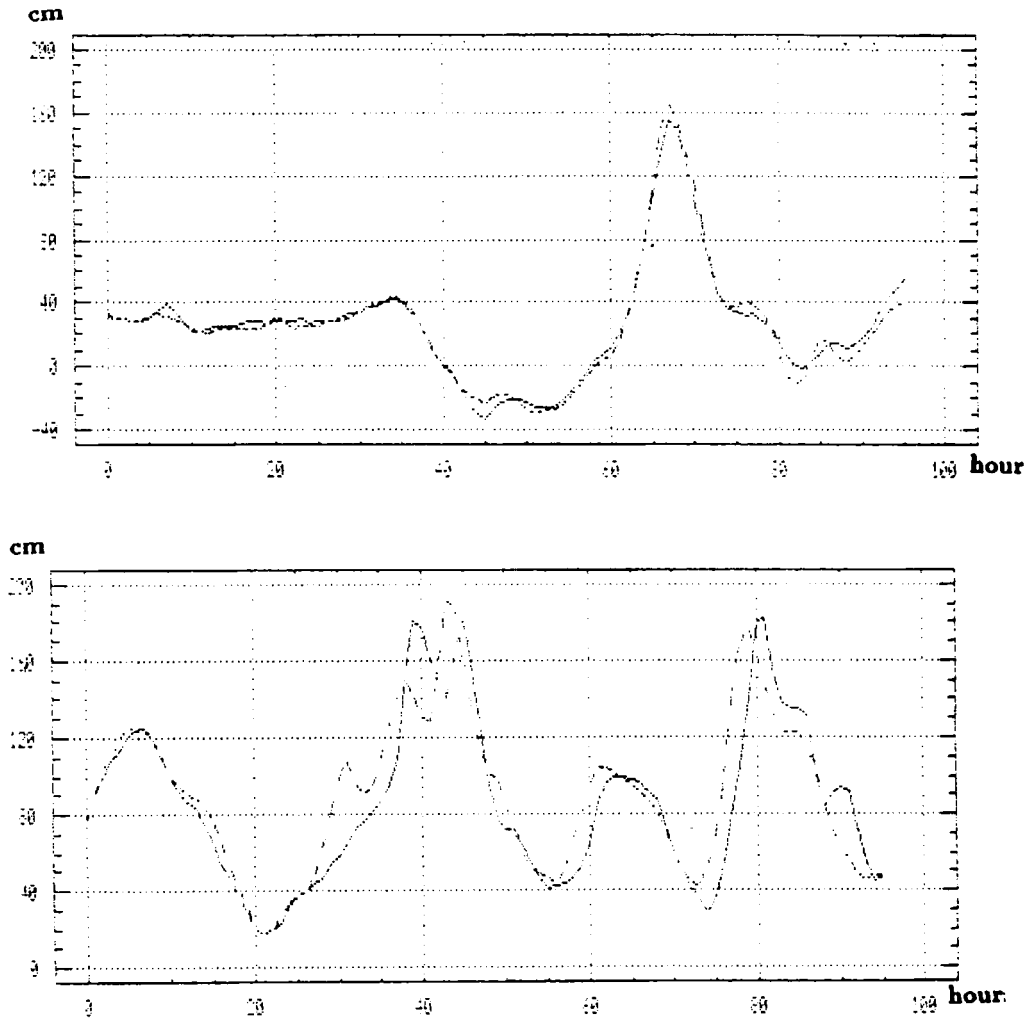

Figure 6. Variations in surface elevation at Strelna during 12–22 October 1981 (top) and 1–4 December 1986 (bottom): solid curves, computations; dashed curves, observed data

(after 240 h). Figure 7a corresponds to the dam conditions with the NTP and SWTP outfalls located near the shores as suggested now. It is seen that in this case the plume from the NTP outfalls flows in the shallow near-shore waters of the north coast. The plume from the SWTP outfalls comes to the south coastal zone with slow water velocities and also flows near the shore. If the dam were to be destroyed as suggested by some public groups, the pollution of coastal regions would only change insignificantly (Figure 7b) according to our results on the water dynamics. The dam prevents plume movement to Sestroretsk but increases concentrations in the inner region adajacent to the dam. On the other hand, the transfer of the NTP outfalls 2 km offshore would result in the plume flowing through the second sluice from the north coast and the north coast would be washed by prognostically purer Neva water (Figure 7c). The transfer of the SWTP outfalls 2 km to the north of the Sea Strait dykes would result in the plume

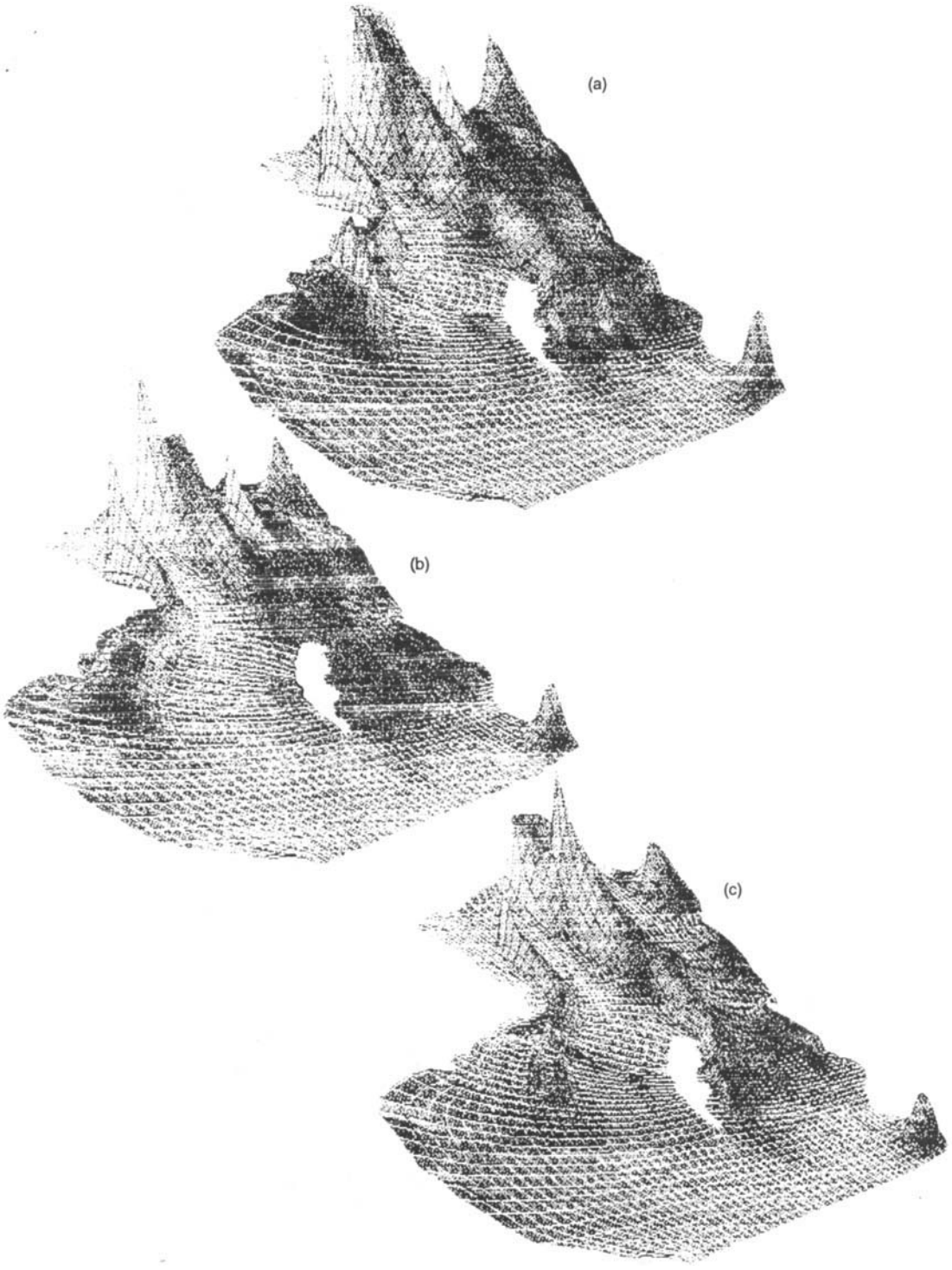

Figure 7. Field of pollutant concentrations in Neva Bay at steady state: a, b, main outfalls located as suggested now, a—dam conditions, b—natural conditions; c, main outfalls transferred farther offshore, dam conditions

flowing along the deep Sea Strait together with the plume from the CTP outfalls to the south of Kotlin Island. A large zone of poor water quality is located near the stagnant zone to the north-east of the Sea Strait dykes owing to the CTP outfalls. The Petrodvoretz, Lomonosov, Strelna and Bolshaia Izora treatment plant outfalls are situated in a very shallow water area with slow water velocities. Thus these outfalls, despite their low discharging capacities, will cause high coli-bacteria concentrations in this region.

The results obtained for the case or unsteady dynamics[28] confirm these conclusions. A review of the temporal variability of the total amount of pollutants in Neva Bay showed that it decreases at times of low surface level in the Gulf of Finland. The computations have shown that the future pollution of the Neva Bay coasts is strongly dependent on the location of the main treatment plant outfalls, but destruction of the dam would not greatly improve the ecological situation in the region.

The next example of a model application is the computation of currents in the Amur river near Khabarovsk city (Figure 8). In recent years human activity and natural river development have led to considerable changes in the river bed in this region. As a result, many hydrotechnical structures now work under adverse conditions. In addition, an exploration of the sand in the main river bed is planned. Computations were performed to estimate the influence of sand-bar development on the hydraulic regime.

The time step was equal to 10 s and the grid consisted of 31 × 107 points. The length of domain was equal to 18 km. A discharge of 19,000 $m^3 s^{-1}$ in the upper open part of the river boundary was assigned. The condition of 'free exit' was assigned in its lower part. Firstly, the model was run with natural morphometry and bathymetry. The Mannings number n was chosen equal to 0·032 according to natural data. The computation showed that a reasonable value of

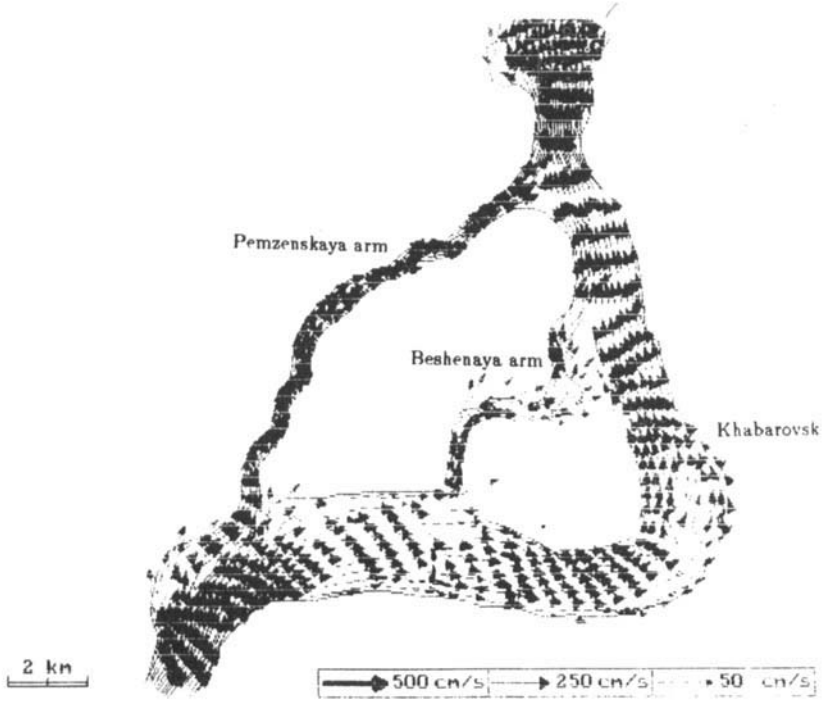

Figure 8. Computed flow in Amur river near Khabarovsk city and proposed location of a sand-bar (dashed curve)

the wall friction coefficient l_w lies in the range 0·2–0·7. After that, many model runs were done with various proposals of morphometry and bathymetry. The most effective one was determined. It was shown that if a sand-bar were situated just opposite the source of the Beshenaya ('Wild') arm, then the water discharge through the main river arm would be the largest and the discharge through the Beshenaya arm would be relatively small. In this case the work of hydrotechnical structures situated on the shores of the main river arm would be improved. The small discharge through the Beshenaya arm would be beneficial, also because the load of sediment materials from its mouth would be diminished.

The results demonstrate the possibilities of the curvilinear co-ordinate method to satisfy the increasingly stringent requirements for modelling coastal zone and inland hydrodynamic and hydroecological processes.

ACKNOWLEDGEMENTS

The authors are grateful to the reviewers for their helpful comments. They also wish to thank Dr. G. V. Stefanofich of the B. E. Vedeneev Hydrotechnical Institute for supplying the results of the hydraulic modelling and Dr. L. Yu. Preobragensky of the State Hydrological Institute for providing the field data on Neva Bay. The authors are grateful to Mrs. H. V. Smirnova of the River Transport Design Institute in St. Petersburg who carried out the application of the model to the Amur river for supplying the results and very helpful discussions.

APPENDIX: GENERAL DESCRIPTION OF MODELLING SYSTEM DESIGN

Based on the methods described above, a software package for the modelling of flows, surface elevations and transport of pollutants in an arbitrary domain has been developed. It is named *Cardinal* (Coastal ARea Dynamics INvestigation ALgorithm). *Cardinal* is developed especially for application on personal computers. The package is written in *Pascal*. Its volume is about 850 kbytes, but only 10% of its code performs computations. The remainder of the package comprises various subroutines aimed at implementing a user-friendly interface and allowing one to display the computational results in different ways. *Cardinal* is divided into 16 separate panels, each solving a particular problem. We give below a brief description of this package.

The first panel (*Name*) carries out the usual file operations (save, load data files). Various types of data such as depths, grid co-ordinates, river information, etc. are saved in different files. Thus it is possible to compose a desired configuration of data files.

The next panel (*Area*) is intended for the generation of domain boundaries by introducing their points with a cursor, mouse or digitizer. The contours may be of two types: closed (main outer contour, islands, semi-islands) or unclosed (e.g. dams). For standard geometrical elements (straight line, circle, rectangle) contour generation is done in a simplified way. Any contour can be eliminated, transferred, rotated or changed in size. The programme can perform image magnification on the screen. It is possible to display the entire computational domain or a small fragment of it. The final size of array of contour points is not known *a priori* and it is not possible to declare it in the computer code. To solve this problem, we declare each point in Pascal as a record consisting of its corresponding (x, y)-co-ordinates and the computer addresses of two records of neighbouring points. When introducing a point or deleting it, a procedure of changing the addresses of neighbouring points is implemented. A similar arrangement is made for the sequence of contours: each contour corresponds to a record variable consisting of the address of the first contour point, the addresses of two neighbouring contours and some other information.

After the domain boundary has been constructed, it is possible to enter the *Grid* panel to generate the curvilinear grid. Prior to grid generation the programme makes several tests of the contours. Once an error is revealed (intersection of lines, too small a number of grid points in the outer contour to set internal ones, incorrect topology, etc.), the programme reports the error and returns to the *Area* panel. If there are no errors, the programme starts the grid generation. This is an iterative process which may be interrupted when it is seen that the grid has been generated or it is necessary to return to the *Area* panel to correct the position of some points. For multiply connected domains the grid generation is performed in two steps. In the first step the grid is generated without taking into account the internal contours. Then the programme ties the first angular point of each internal closed contour to the nearest grid point. For the unclosed contours it is necessary to tie two (e.g. first and last) points of each contour. These tied points can be changed by the user. In the second step the grid is generated with cut-outs for the internal contours.

The next step is the input of the depth field. The depths can be introduced directly at the curvilinear grid points, but often it is more convenient to introduce them first at the points of a rectangular grid and then interpolate to the points of the curvilinear grid. A rectangular grid with arbitrary space steps is then constructed first. This grid may be rotated. If the depth data for the given basin are available from some text file, *Cardinal* can read this file irrespective of the format in which these data are presented. Finally, if the depth field is expressed analytically, then *Cardinal* can read the equation and after internal translation introduce the depths accordingly to it.

As described in Section 3, three types of open boundaries may be suggested and the next three panels deal with these open bounary types. The *Rivers* panel is intended for introducing all data about rivers, i.e. sections of open boundary with given discharges. For each river the discharges can be assigned either in the form of a data row or in the form of an analytical equation. The pollution concentrations in each river can also be specified. The *Levels* panel is intended to introduce the sections of open boundary with given values of surface level variations. The time histories of surface level may be specified separately for two opposite shores and may also be given using an analytical expression. In the *Free exit* panel a user may assign the sections of open boundary through which long waves can leave the computational domain.

A separate panel (*Parameters*) is used for empirical coefficients: lateral turbulent eddy coefficient μ_l, lateral turbulent diffusivity μ_c, non-conservativity λ and geographical latitude. The computational regime is also chosen here: only dynamics, or only transport pollutants with given dynamics or both.

In the *Wind* panel the wind is assigned in the form of time series of wind velocities and directions with a given time step or in the form of an arbitrary analytical dependence. In the latter case the wind can also be space-dependent. The analytical formula for wind stress coefficients k_w may be assigned here.

The next panel (*Sources*) assigns the internal pollution sources. The process includes the choice of their locations, discharges and concentrations.

In the *Bottom type* panel different values for the bottom friction coefficient μ may be assigned by dividing the computational domain into a number of regions with constant values of it.

Before starting the computations, it is possible to define the grid points at which the time histories of velocity vectors, surface level oscillations and concentration variations will be recorded. It is also possible to outline the area in which the time history of pollution volume will be recorded. This is performed in the *Mareographs* panel.

At last, after the domain contour and the curvilinear grid have been generated and the depth field, the open boundaries, all the empirical coefficients and the wind have been specified, the

computation may be started in the next (*Computational*) panel. In this panel the time step, the number of steps, the type of picture to be displayed during the computations and some other parameters are defined. The types of graphics available are vector fields of velocity and stream, hatching pictures of surface level and concentration fields, three-dimensional representations of these last fields and graphics of time histories of variables at given points. *Cardinal* implies a reasonable choice of time step to ensure that the CFL number is of the order of unity. However, a larger time step can be assigned, since *Cardinal* uses a semi-implicit scheme in the dynamic computation and the implicit scheme for the advection–diffusion equation. The initial surface level, velocity and concentration fields can be defined analytically. These fields can also be loaded from a file.

The next (*Write results*) panel ensures the recording of all the results in the text file in the form of digital information. Finally the *Quit* panel stops *Cardinal*.

The large percentage of auxiliary procedures in comparison with the computational block is, besides various graphical procedures, due to the requirement to foresee various types of errors that might occur during the construction of the computational domain. For example, when creating the area of computation, it is possible to draw an island outside the area or insert one island into another. Such a situation hardly ever occurs, but an integrated modelling system should be ready to react to arbitrary user actions. To find such an error, the programme calculates the sum of the angles below which all the points of the closed contour are seen from an arbitrary point of the other contour. If the point is situated inside the other contour, the sum of the angles will be equal to 2π, while it will be equal to zero if the point is located outside the contour. After arrangement of the contour sections corresponding to the openings along the boundary, the domain may be expanded in the *Area* panel. As a result, openings may be found inside the domain. A similar situation may occur for the pollution sources: instead of being inside the domain they may occur outside it. Most errors are interlocked: for example, it is not possible to input a negative depth or to introduce two contour points with the same co-ordinates. The presence of other errors such as those mentioned above can only be detected after they have been introduced in the model.

Cardinal can translate analytical formulae in text form and use them in the computation. If a syntactical error occurs in a formula (e.g. unmatched brackets, an unknown function or argument), then *Cardinal* shows the position of the wrong character(s). Besides all the elementary functions, cylindrical and spherical Bessel functions have been introduced in the programme. Bessel functions are encountered when solving various hydrodynamical problems in circular basins for example. The method of continued fractions, which is extremely accurate, is used to calculate these functions. Very often an analytical dependence contains a conditional operator. Such a situation arises, for example, when the initial surface level perturbation needs to be assigned in some subdomain of the computational area. Expressions of this type can be introduced via the θ-function, which is equal to zero for negative arguments and unity for positive arguments. Using products of the θ-functions, any conditional operators can be reproduced. The model is constantly being updated and the incorporation of additional computational possibilities is becoming more convenient and simpler.

REFERENCES

1. J. J. Stoker, *Water Waves*, Interscience, New York, 1953.
2. B. Gustafsson and A. Sundström, 'Incompletely parabolic problems in fluid dynamics', *SIAM J. Appl. Math.*, **35**, 343–357 (1978).

3. G. Pedersen, 'On the effect of irregular boundaries in finite difference models', *Int. j. numer. methods fluids*, **6**, 497–505 (1986).
4. T. J. Weare, 'Errors arising from irregular boundaries in ADI solutions of the shallow-water equations', *Int. j. numer. methods eng.*, **14**, 921–931 (1979).
5. I. M. Navon, 'A review of finite-element methods for solving shallow-water equations', in B. A. Schrefler and O. C. Zienkiewicz (eds), *Proc. Int. Conf. on Computer Modeling in Ocean Engineering*, Balkema, Rotterdam, 1988, pp. 273–278.
6. C. Goto and N. Shuto, 'Numerical computation of borelike tsunamis in a curved river', *Proc. 5th Conf. on Ocean Engineering in Republic of China*, 1981, pp. 125–142.
7. J. F. Thompson, F. C. Thames and C. W. Mastin, 'TOMCAT—a code for numerical generation of boundary-fitted curvilinear coordinate systems on fields containing any number of arbitrary two-dimensional bodies', *J. Comput. Phys.*, **24**, 274–302 (1977).
8. B. H. Johnson, 'Numerical modeling of esturaine hydrodynamics on a boundary-fitted coordinate system', in J. F. Thompson (ed.), *Numerical Grid Generation*, North-Holland, Amsterdam, 1982, pp. 409–436.
9. J. Haeuser, H. -G. Paap, D. Eppel and A. Mueller, 'Solution of shallow water equations for complex flow domains via boundary-fitted coordinates', *Int. j. numer. methods fluids*, **5**, 727–744 (1985).
10. N. E. Voltzinger and K. A. Klevanny, 'Integration of three-dimensional motion equations in arbitrary region for compuation of flood', *Izv. Acad. Sci. USSR Atmos. Ocean. Phys.*, **23**, 462–469 (1987).
11. A. G. L. Borthwick and R. W. Barber, 'River and reservoir flow modeling using the transformed shallow water equations', *Int. j. numer. methods fluids*, **14**, 1193–1217 (1992).
12. M. L. Spaulding, 'A vertically averaged circulation model using boundary-fitted coordinates', *J. Phys. Oceanogr.*, **14**, 973–982 (1984).
13. J. C. Swanson, M. Spaulding, J. -P. Mathisen and Ø. O. Jenssen, 'A three dimensional boundary fitted coordinate hydrodynamic model, Part I: Development and testing', *Deutsche Hydrogr. Z.*, **42**, 169–186 (1989).
14. N. E. Voltzinger, K. A. Klevanny and E. N. Pelinovsky, *Long-wave dynamics of Coastal Zone*, Gidrometeoizdat, Leningrad, 1989 (in Russian).
15. Y. P. Sheng, 'On modeling three-dimensional estuarine and marine hydrodynamics', in J. Nihoul, (ed.), *Three-dimensional models of Marine and Estuarine Dynamics*, Elsevier, Amsterdam, 1988, pp. 35–54.
16. T. Elvius and A. Sundström, 'Computational problems related to limited-area modeling', *WMO GARP Publ. Ser.*, **17**, 379–416 (1979).
17. A. Robert, 'Semi-implicit method', *WMO GARP Publ. Ser.*, **17**, 419–437 (1979).
18. V. Casulli and F. Notarnicola, 'An Eulerian–Lagrangian method for tidal current computation', in B. A. Schrefler and O. C. Zienkiewicz (eds.), *Proc. Int. Confer. on Computer Modelling in Ocean Engineering*, Balkema, Rotterdam, 1988 pp. 237–244.
19. J. H. Mahaffy, 'A stability-enhancing two-step method for fluid flow calculation', *J. Comput. Phys.*, **46**, 329–341 (1982).
20. J. Glekas, G. Bergeles and N. Athanassiadis, 'Numerical solution of the transport equation for passive contaminants in three-dimensional complex terrains', *Int. j. numer. methods fluids*, **7**, 319–335 (1987).
21. C. -D. Munz, 'On the numerical dissipation of high resolution schemes for hyperbolic conservation law', *J. Comput. Phys.*, **77**, 18–39 (1988).
22. H. -O. Kreiss. 'Initial boundary value problems for hyperbolic systems', *Commun. Pure Appl. Math.*, **22**, 277–298 (1970).
23. F. Mesinger and A. Arakawa,'Numerical methods used in atmospheric models', *WMO GARP Publ. Ser.*, **1**, (1976).
24. S. S. Abarbanel and E. M. Murman, 'Stability of two-dimensional hyperbolic initial boundary value problems for explicit and implicit schemes', *J. Comput. Phys.*, **48**, 160–167 (1982).
25. B. Gustafsson, H. -O. Kreiss and A. Sundström, 'Stability theory of difference approximation for mixed initial boundary–value problem', *Math. Comput.*, **26**, 649–686 (1972).
26. H. Lamb, *Hydrodynamics*, Dover, New York, 1945.
27. I. M. Navon and H. A. Riphagen, 'An implicit compact fourth-order algorithm for solving the shallow-water equations in conservation law form', *Mon. Weather Rev.*, **107**, 1107–1127 (1979).
28. K. A. Klevanny, L. Y. Preobrazhensky, N. E. Voltzinger and A. V. Zolnikov, 'Body-fitted coordinates for calculating long-wave disturbances and impacts of coastal engineering structures on the hydrodynamic and pollution regimes', *Proc. 3rd Int. Conf. on Coastal and Port Engineering in Developing Countries*, Vol. 2, 1991, pp. 1311–1320.